Amplification on a relativistic electron beam in a spatially periodic transverse magnetic field

Ira B. Bernstein and J. L. Hirshfield
Mason Laboratory, Yale University, New Haven, Connecticut 06520
(Received 12 April 1979)

An exact solution is given for the canonical model equations describing the electromagnetic fields on a free-electron-laser amplifier comprised of a high-quality relativistic electron beam propagating along the axis of a helical pump magnetic field. The case of a cold beam is analyzed in detail and it is shown that, depending upon the parameters, one can have gain when the system is stable, owing to constructive spatial interference of modes, or exponential gain when it is unstable. Gain curves, line shapes, and linewidths are presented for conditions of reported and planned experiments. Reasonable agreement is found with the reported experiments.

I. INTRODUCTION

A considerable body of literature[1] has accumulated in the past few years on wave propagation on a beam of relativistic electrons undulating in a spatially periodic transverse static magnetic field. That work has been largely motivated by experiments in which near-infrared radiation was generated[2] and amplified[3] when electron beams with energies in the range 20–50 MeV traversed a 5.2-m-long periodic transverse magnetic field set up by a bifilar double-helix winding. More recent experiments[4] employing an intense (25 kA) lower-energy beam (1.5 MeV) have demonstrated that megawatt-level radiation at submillimeter wavelengths can be generated as well. These successes have stimulated the design of further intense beam experiments,[5] with the objectives of increased power and efficiency. Other proposals to design efficient tunable sources of visible radiation using beams with energies up to 100 MeV have also been presented.[6] Great practical interest would attach to these experiments, if one could thereby demonstrate that the accessible range of wavelength, power, and efficiency with this interaction went beyond what is available from molecular gas lasers.[7] The additional property of electronic tunability inherent in the "free-electron-laser" interaction discussed here is of course absent in most molecular laser systems.

The purpose of this paper is to present an exact solution for a theoretical model of an idealized amplifier configuration patterned after the experiments. The important features of this analysis are as follows.

(a) The transverse momentum undulations of the electrons are included exactly in the equilibrium electron distribution function. The theory is thus exact for finite undulations of any magnitude.

(b) The electromagnetic response of the electron beam is determined by a linearization of the kinetic equation. No multiple expansions are required since the stationary undulations are included in the equilibrium. Interpretations in terms of nonlinear physical mechanisms involving stimulated scattering and the like[8] are thus not essential to a full description.

(c) A system of basis vectors with the symmetry of the helical undulations is introduced which permits solution of the problem by Laplace transformation. The normal modes of this system are neither plane transverse electromagnetic waves nor longitudinal electrostatic beam plasma waves and thus cannot be obtained by conventional transform methods in a system with constant basis vectors. Determination of mode polarization is a routine matter in the natural coordinates.

(d) Exact steady-state solutions for the linearized radiation field of the form

$$\vec{E}(z,t)=\sum_{j=1}^{6}\vec{a}_j e^{i(k_j z-\omega t)}$$

are obtained, where the $k_j(\omega)$ are (sometimes complex) independent roots of a sixth-order algebraic dispersion relation and the $a_j(\omega)$ are linearly independent mode amplitudes.

(e) Analysis of the dispersion relation, under conditions appropriate for an amplifier, permits the approximate reduction of the problem to an equation of the form

$$(k-k_6)(k-k_5)(k-k_4)G(k)=0\,,$$

where $G(k)$ is a cubic equation in k. The range of parameters where this cubic possesses complex roots is readily identified, as is the value of the maximum spatial growth constant. Under representative conditions we demonstrate that the parameters traverse the regimes of complex as well as real roots, so that previously employed[9] simplified limiting forms for the gain coefficient are not generally applicable.

(f) Two of the six modes have negative phase and

group velocity and thus have zero amplitude in an amplifier with an ideal output coupler (i.e., one with no reflections). Since at most one of the remaining four modes can exhibit exponential growth (complex root), the output amplitude of a high-gain amplifier is shown to be only about one-sixth what it would be if the growing mode were propagating alone. (This corresponds to an input coupling loss of 15.6 dB.)

(g) Gain curves have been obtained for conditions of the reported[3] amplifier experiment. Reasonable agreement between theory and experiment as to gain, line shape, and linewidth is found. The regime of complex roots contributes not insignificantly to the gain function, but under interesting circumstances one can obtain gain due to constructive interference even when there are no complex roots. Gain curves are also presented for conditions of a planned experiment using an intense beam.

II. THEORY

Consider an electromagnetic field that depends only on time t and the coordinate z. It can be represented in terms of potentials

$$\vec{A} = \vec{e}_x A_x(z,t) + \vec{e}_y A_y(z,t)$$

and (1)

$$\Phi = \Phi(z,t),$$

such that

$$\vec{B} = \nabla \times \vec{A} = -\vec{e}_x \partial A_y/\partial z + \vec{e}_y \partial A_x/\partial z , \tag{2}$$

$$\vec{E} = -\nabla\Phi - c^{-1}\partial\vec{A}/\partial t$$

$$= -\vec{e}_x c^{-1}\partial A_x/\partial t - \vec{e}_y c^{-1}\partial A_y/\partial t - \vec{e}_z \partial\Phi/\partial z . \tag{3}$$

On using Maxwell's equations it is readily seen that the potentials obey the equations

$$\partial^2\vec{A}/\partial z^2 - c^{-2}\partial^2\vec{A}/\partial t^2 = -(4\pi/c)(\vec{e}_x J_x + \vec{e}_y J_y), \tag{4}$$

$$\partial^2\Phi/\partial z\,\partial t = 4\pi J_z , \tag{5}$$

where $\vec{J}$ is the current density.

Let the velocity of an electron be $\dot{\vec{r}}$ and define

$$\vec{u} = \gamma\dot{\vec{r}}/c , \tag{6}$$

$$\gamma = (1+u^2)^{1/2} . \tag{7}$$

Then the equation of motion can be written

$$\dot{\vec{u}} = -(e/mc)(\vec{E} + \vec{u}\times\vec{B}/\gamma), \tag{8}$$

where m is the rest mass, and it can readily be seen that

$$\alpha = u_x - eA_x/mc^2 \quad \text{and} \quad \beta = u_y - eA_y/mc^2 \tag{9}$$

are particle constants of the motion. Moreover, the scalar product of Eq. (8) with $\gamma\vec{u}$ leads to

$$u\dot{u} = \gamma\dot{\gamma} = -e\vec{E}\cdot\vec{u}/mc . \tag{10}$$

Now consider an electron distribution function f which depends only on the Cartesian coordinates $z, \dot{x}, y, \dot{z}$, and t. If in place of these one employs rather the set α, β, u, z, and t, then the Vlasov equation reduces to

$$0 = \dot{f}$$

$$= \partial f/\partial t + \dot{z}\,\partial f/\partial z + \dot{\alpha}\,\partial f/\partial\alpha + \dot{\beta}\,\partial f/\partial\beta + \dot{u}\,\partial f/\partial u$$

$$= \partial f/\partial t + \dot{z}\,\partial f/\partial z - (e\vec{E}\cdot\vec{u}/mcu)\partial f/\partial u , \tag{11}$$

since $\dot{\alpha} = 0, \dot{\beta} = 0$, and $\dot{u}$ is given by Eq. (10). In Eq. (11),

$$\dot{z} = \frac{c}{\gamma}\left[u^2 - \left(\beta + \frac{eA_y}{mc^2}\right)^2 - \left(\alpha + \frac{eA_x}{mc^2}\right)^2\right]^{1/2} , \tag{12}$$

$$\vec{u} = \left(\frac{\gamma\dot{z}}{c}\right)\vec{e}_z + \left(\beta + \frac{eA_y}{mc^2}\right)\vec{e}_y + \left(\alpha + \frac{eA_x}{mc^2}\right)\vec{e}_x . \tag{13}$$

Consider a time-independent state in which the beam density is so small that the self-electric and magnetic fields may be approximated as zero. The associated solution of Eq. (11) is then $f_0(\alpha,\beta,u)$. When perturbations about this steady state are small it is convenient to write $f = f_0 + f_1 + \cdots$, $\vec{E} = 0 + \vec{E}$, $\vec{B} = \vec{B}_0 + B_1$, etc. Then on linearization Eq. (11) yields

$$\partial f_1/\partial t + \dot{z}_0\partial f_1/\partial z = (e\vec{E}_1\cdot\vec{u}_0/mcu)\partial f_0/\partial u , \tag{14}$$

where

$$\dot{z}_0 = \frac{c}{\gamma}\left[u^2 - \left(\beta + \frac{eA_{0y}}{mc^2}\right)^2 - \left(\alpha + \frac{eA_{0x}}{mc^2}\right)^2\right]^{1/2} , \tag{15}$$

$$\vec{u}_0 = \left(\frac{\gamma\dot{z}_0}{c}\right)\vec{e}_z + \left(\beta + \frac{eA_{0y}}{mc^2}\right)\vec{e}_y + \left(\alpha + \frac{eA_{0x}}{mc^2}\right)\vec{e}_x . \tag{16}$$

Formulation of the problem in this manner thus includes the effects of the z-varying static magnetic field exactly, and permits a solution using first-order perturbation theory. No expansions in powers of $\vec{A}_0$ are required.

Therefore, let us seek solutions of the linearized equations of the form $\vec{E}_1 = \mathrm{Re}\vec{a}(z)e^{-i\omega t}$, $\vec{J}_1 = \mathrm{Re}\vec{j}(z)e^{-i\omega t}$, $f_1 = \mathrm{Re}F(\alpha,\beta,u,z)e^{-i\omega t}$, etc. Then if

$$\vec{a}_1 = a_x\vec{e}_x + a_y\vec{e}_y , \tag{17}$$

it follows from Eqs. (2)–(5) that

$$\vec{a}_1'' + \omega^2\vec{a}_1/c^2 = 4\pi i\omega\vec{j}_1/c^2 , \tag{18}$$

$$a_z = -4\pi i j_z/\omega , \tag{19}$$

where a prime denotes a derivative with respect to z. Equation (14) then becomes

$$F' - i(\omega/\dot{z}_0)F = (e\vec{a}\cdot\vec{u}_0/mcuz_0)\partial f_0/\partial u , \tag{20}$$

the solution of which is

$$F(\alpha,\beta,u,z,)\exp[i\psi(\alpha,\beta,u,z)]-F(\alpha,\beta,u,0)$$
$$=(e/mcu)[\partial f_0(\alpha,\beta,u)/\partial u]\int_0^z dz'\exp[i\psi(\alpha,\beta,u,z')]\vec{a}(z')\cdot\vec{u}_0(\alpha,\beta,u,z')/\dot{z}_0(\alpha,\beta,u,z'), \quad (21)$$

where

$$\psi(\alpha,\beta,u,z)=\omega\int_0^z dz'/\dot{z}_0(\alpha,\beta,u,z'). \quad (22)$$

The current density $\vec{J}$ for an unneutralized beam is

$$\vec{J}=-e\int d^3u\,\vec{u}cf/\gamma=-e\int d\alpha\,d\beta du\vec{u}cf/\gamma u_z, \quad (23)$$

where $u_z=\gamma\dot{z}/c$ and $\dot{z}$ is given by Eq. (12). The first-order part of Eq. (23) yields

$$\vec{j}=-e\int d\alpha\,d\beta\,du\,(uc/\gamma)(-i(e\vec{a}_\perp/mc\omega u_{0z})f_0-(u_{1z}/u_{0z}^2)[\vec{e}_x(\alpha+eA_{0x}/mc^2)+\vec{e}_y(\beta+eA_{0y}/mc^2)]f_0$$
$$+[\vec{e}_x(\alpha+eA_{0x}/mc^2)/u_{0z}+\vec{e}_y(\beta+eA_{0y}/mc^2)/u_{0z}+\vec{e}_z]F), \quad (24)$$

where

$$u_{0z}u_{1z}=i(ea_x/mc\omega)(\alpha+eA_{0x}/mc^2)+i(ea_y/mc\omega)(\beta+eA_{0y}/mc^2). \quad (25)$$

There is one case which can be solved exactly, viz., where

$$f_0=\delta(\alpha)\delta(\beta)g(u), \quad (26)$$
$$F(\alpha,\beta,u,0)=\delta(\alpha)\delta(\beta)G(u), \quad (27)$$

and

$$\vec{A}_0(z)=-(B_0/k_0)(\vec{e}_x\cos k_0z+\vec{e}_y\sin k_0z). \quad (28)$$

One notes that $A_0^2=$ const, and that

$$\vec{B}_0=\nabla\times\vec{A}_0=B_0(\vec{e}_x\cos k_0z+\vec{e}_y\sin k_0z), \quad (29)$$

which corresponds to the magnetic field near the axis of a system of helical coils carrying no net current. This is the conventional zero-order-model magnetic field adopted in free-electron-laser theory. It is convenient to introduce coordinates which track the vector potential. The basis vectors are

$$\vec{e}_1=-\vec{e}_x\cos k_0z+\vec{e}_y\cos k_0z,\quad \vec{e}_2=-\vec{e}_x\cos k_0z-\vec{e}_y\sin k_0z,\quad \vec{e}_3=\vec{e}_z. \quad (30)$$

Then Eq. (24) leads to

$$\vec{j}=-e\int du\left\{-i\left(\frac{eug}{m\omega\gamma u_{0z}}\right)\vec{a}_\perp-i\left(\frac{eu\xi^2g}{m\omega\gamma u_{0z}^3}\right)\vec{e}_2\vec{e}_2\cdot\vec{a}_\perp+\left(\frac{\xi\vec{e}_2(z)}{u_{0z}}+\vec{e}_3\right)\exp\left(\frac{i\omega\gamma z}{u_{0z}c}\right)\right.$$
$$\left.\times\left[\frac{cuG}{\gamma}+\frac{e}{mc}\frac{dg}{du}\int_0^z dz'\,\vec{a}_\perp(z')\cdot\left(\frac{\xi\vec{a}_2(z')}{u_{0z}}+\vec{e}_3\right)\exp\left(\frac{-i\omega\gamma z'}{u_{0z}c}\right)\right]\right\}, \quad (31)$$

where $\xi=-eB_0/mc^2k_0$. Now it is seen that $u_{0z}=(u^2-\xi^2)^{1/2}$ is independent of z, and $\psi(0,0,u,z)=\omega\gamma z/u_{0z}c$.

Equation (31) can be employed to deal with the effects of a thermal distribution in $\dot{z}$. We shall, however, limit ourselves to a cold beam, viz.,

$$g(u)=N_0\delta(u-u'), \quad (32)$$
$$G(u)=N_1\delta(u-u'). \quad (33)$$

If we then introduce the plasma frequency $\omega_p=(4\pi N_0e^2/m)^{1/2}$ and write

$$\vec{a}=a_1\vec{e}_1+a_2\vec{e}_2+a_3\vec{e}_3, \quad (34)$$

then Eqs. (31), (19), and (18) can be reduced to

$$a_1''+(\omega^2/c^2-k_0^2)a_1-2k_0a_2'=(\omega_p^2u/c^2\gamma u_{0z})a_1, \quad (35)$$
$$a_2''+\left(\frac{\omega^2}{c^2}-k_0^2\right)a_2+2k_0a_1'=\frac{\omega_p^2}{c^2}\left[\frac{u}{\gamma u_{0z}}a_2+\frac{\xi^2u}{\gamma u_{0z}^3}a_2-i\frac{\omega}{c}\frac{\partial}{\partial u}\int_0^z dz'\left(\frac{\xi^2a_2(z')}{u_{0z}^2}+\frac{\xi a_3(z')}{u_{0z}}\right)\exp\left(\frac{i\omega\gamma(z-z')}{u_{0z}c}\right)\right]$$
$$+\frac{4\pi i\omega euN_1\xi}{\gamma cu_{0z}}\exp\left(\frac{i\omega\gamma z}{u_{0z}c}\right), \quad (36)$$

$$a_3 = -i\frac{\omega_p^2}{\omega c}\frac{\partial}{\partial u}\int_0^z dz'\left(\frac{\xi a_2(z')}{u_{0z}} + a_3(z')\right)\exp\left(\frac{i\omega\gamma(z-z')}{u_{0z}c}\right), \tag{37}$$

where we have suppressed the prime on the u' of Eqs. (33) and (34).

Note that Eqs. (35)–(37) are a system of integro-differential equations where the integrals are of the convolution type and the coefficients of the other terms are constants. This latter property is not enjoyed by the corresponding equations for a_x, a_y, and a_z. The set (35)–(37) can be readily solved by a Laplace transformation. In other words, if one defines

$$\alpha_j(k) = \int_0^\infty dz\, a_j(z)e^{-ikz} \quad (j=1,2,3), \tag{38}$$

where Imk is sufficiently negative to ensure convergence, and defines

$$\lambda = kc/\omega - \gamma/u_{0z}, \tag{39}$$

then on employing the convolution theorem, Eqs. (35)–(37) are carried into

$$\epsilon_{11}\alpha_1 - \left(\frac{2ik_0kc^2}{\omega^2}\right)\alpha_2 = \frac{c^2}{\omega^2}[a_1'(0) + ika_1(0) - 2ik_0a_2(0)], \tag{40}$$

$$\left(\frac{2ik_0kc^2}{\omega^2}\right)\alpha_1 + \epsilon_{22}\alpha_2 + \epsilon_{33}\alpha_3 = \frac{c^2}{\omega^2}[a_2'(0) + ika_2(0) + 2ik_0a_1(0)], \tag{41}$$

$$\epsilon_{32}\alpha_2 + \epsilon_{33}\alpha_3 = \frac{c^2}{\omega^2\lambda}\frac{4\pi N_1 eu}{\gamma}, \tag{42}$$

where

$$\epsilon_{11} = 1 - \frac{c^2}{\omega^2}(k^2+k_0^2) - \frac{\omega_p^2}{\omega^2}\frac{u}{\gamma u_{0z}}, \tag{43}$$

$$\epsilon_{22} = 1 - \frac{c^2}{\omega^2}(k^2+k_0^2) - \frac{\omega_p^2}{\omega^2}\frac{u}{\gamma u_{0z}^3}\left(u^2 + \frac{2\gamma\xi^2}{\lambda u_{0z}} + \frac{\xi^2(1+\xi^2)}{\lambda^2 u_{0z}^2}\right), \tag{44}$$

$$\epsilon_{23} = \epsilon_{32} = -\frac{\omega_p^2}{\omega^2}\frac{u}{\gamma u_{0z}^3}\left(\frac{\gamma\xi}{\lambda} + \frac{\xi(1+\xi^2)}{\lambda^2 u_{0z}}\right), \tag{45}$$

$$\epsilon_{33} = 1 - \frac{\omega_p^2}{\omega^2}\frac{u}{\gamma u_{0z}^3}\frac{1+\xi^2}{\lambda^2}. \tag{46}$$

If one eliminates α_1 and α_3, Eqs. (43)–(45) yield

$$R\alpha_2 = \lambda^2\epsilon_{11}\epsilon_{33}\left(a_2'(0) + ika_2(0) + 2ik_0a_1(0) + \frac{4\pi N_1 eu\xi}{\gamma u_{0z}\lambda}\right)\frac{c^2}{\omega^2} - \frac{2ik_0kc^2}{\omega^2}\lambda^2\epsilon_{33}[a_1'(0) + ika_1(0) - 2ik_0a_2(0)]\frac{c^2}{\omega^2}$$
$$- \frac{4\pi N_1 eu}{\gamma\lambda}\epsilon_{11}\epsilon_{23}\frac{c^2}{\omega^2}, \tag{47}$$

where

$$R = \lambda^2[\epsilon_{11}(\epsilon_{22}\epsilon_{33} - \epsilon_{23}^2) - 4(k_0^2k^2c^4/\omega^4)\epsilon_{33}]. \tag{48}$$

If one uses the identity

$$(\epsilon_{22} + x_0^2)\epsilon_{23} - \epsilon_{23}^2 = (\epsilon_{11} + x_0^2)(\epsilon_{33} + \xi^2\delta^2/\lambda^2), \tag{49}$$

one can write Eq. (48) in the form

$$R = [(x-\mu)^2 - \delta^2(1+\xi^2)][b^2 - (x+x_0)^2][b^2 - (x-x_0)^2] + \xi^2\delta^2(b^2-x^2)(b^2-x^2-x_0^2), \tag{50}$$

where

$$x = kc/\omega, \quad x_0 = k_0c/\omega, \quad \delta = (\omega_p/\omega)(u/\gamma u_{0z}^3)^{1/2}, \quad b = (1-u_{0z}^2\delta^2)^{1/2}, \quad \mu = \gamma/u_{0z}. \tag{51}$$

In the limit $x_0 \to 0$, Eq. (50) corresponds to the result found by Bernstein and Hirshfield[10] in the geometric optics approximation. One can also write Eq. (50) as

$$R = \prod_{j=1}^{6}(x - x_j),$$

where the x_j are the roots of $R = 0$.

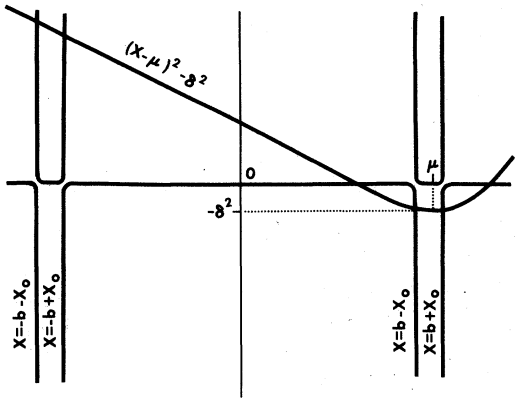

FIG. 1. Graphical representation of the dispersion relation (55). Six real roots result when the left-hand side $l(x)=(x-\mu)^2-\delta^2$ has six intersections with the right-hand side $r(x)$ (discontinuous curve).

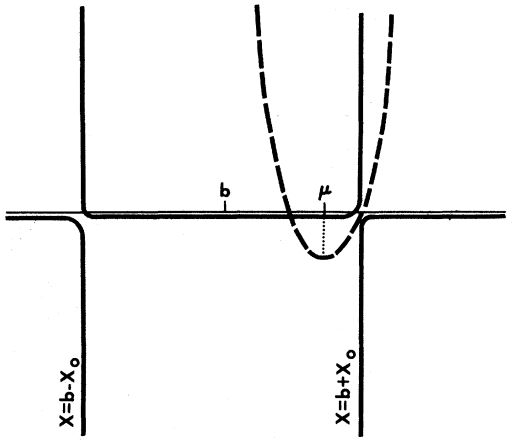

FIG. 2. Graphical representation of the dispersion relation (55) near $x=b+x_0$. In this case $l(x)$ (dashed cure) only has four intersections with $r(x)$ (off scale on this plot) since $l(x)$ has slipped through the gap in $r(x)$. Two complex conjugate roots result, one corresponding to exponential spatial growth.

The transforms α_j are readily seen to be analytic functions of k, and hence of x, everywhere except at the points $kc/\omega=x=x_j$, where there are simple poles. Thus the Bromwich inversion integral

$$a_j=\left(\frac{1}{2\pi i}\right)\int dk\,\alpha_j e^{ikz}$$
$$=\left(\frac{1}{2\pi i}\right)(\omega/c)\int dx\,\alpha_j\exp(i\omega zx/c) \tag{52}$$

can be evaluated in terms of the residues of the integrand. In other words, if one writes $R'=dR(x)/dx$, defines

$$\hat{a}=4\pi N_1 euc\xi\delta^2/\omega\gamma u_{0z},$$

and introduces

$$B(x)=\frac{\omega\alpha_2}{c}R=(b^2-x_0^2-x^2)\left[[(x-\mu)^2-\delta^2(1+\xi^2)]\left(\frac{c}{\omega}a_2'(0)+ixa_2(0)+2ix_0a_1(0)\right)+(\gamma u_{0z}+x-\mu)\hat{a}\right]$$
$$-2ix_0x[(x-\mu)^2-\delta^2(1+\xi^2)]\left(\frac{c}{\omega}a_1'(0)+ixa_1(0)-2ix_0a_2(0)\right), \tag{53}$$

there results

$$a_2=\sum_{j=1}^{6}B(x_j)\frac{\exp(ix_j\omega z/c)}{R'(x_j)} \tag{54}$$

and a_1 and a_3 follow from Eqs. (35) and (37).

The dispersion relation $R=0$ is conveniently analysed by writing it in the form obtained from Eq. (50) by subtracting from both sides the rightmost term in Eq. (50), dividing by the factor $[b^2-(x+x_0)^2][b^2-(x-x_0)^2]$, and then adding $\xi^2\delta^2$ to both sides of the equation. After a partial fraction decomposition the result is

$$(x-\mu)^2-\delta^2=-\frac{\xi^2\delta^2x_0}{8b}\left[\frac{4b^2+3x_0b-2x_0^2}{b+x_0}\left(\frac{1}{x-(b+x_0)}-\frac{1}{x+(b+x_0)}\right)-\frac{4b^2-3x_0b-2x_0^2}{b-x_0}\left(\frac{1}{x-(b-x_0)}-\frac{1}{x+(b-x_0)}\right)\right]. \tag{55}$$

For parameters currently accessible experimentally $\delta\ll x_0\ll 1$, $b\simeq 1$, and

$$\mu=\gamma/u_{0z}=(1+u^2)^{1/2}(u^2-\xi^2)^{-1/2}$$
$$\simeq 1+(1+\xi^2)/2\gamma^2\simeq 1. \tag{56}$$

A cross plot of the right- and left-hand sides of Eq. (55) is shown schematically in Fig. 1, where the parabola is the left-hand side and the discontinuous curve the right-hand side. Note that there are six intersections unless the dashed curve passes through a gap in the solid curve. A more precise version of the region near $x=b$ is shown in Fig. 2. When the dashed curve passes through the gap there are four real roots and a pair of complex conjugate roots, one of which corresponds to exponential gain. For the situation represented in Fig. 2 one must have roughly that

$\mu+\delta\simeq b+x_0$ or alternatively $(1+\xi^2)/2\gamma^2\simeq x_0$. This is the familiar ratio of wavelength to helix period for free-electron lasers. The dashed curve in Fig. 1 cannot pass through the gap near $x=b-x_0$ since this would require $\mu-b\simeq b-x_0$ or $(1+\xi^2)/2\gamma\simeq -x_0$. Three of the component waves are slow ($k_z c/\omega>1$).

It is readily seen from Eq. (50) that the two leftmost intersections of Fig. 1 correspond to

$$x_6=-b-x_0+O(\xi^2\delta^2x_0)\,,\qquad x_5=-b+x_0+O(\xi^2\delta^2x_0)\,, \tag{57}$$

and lead to space-time dependences

$$a_2\simeq\exp[i(\omega/c)(z+ct+\cdots)]\,, \tag{58}$$

which are waves propagating backwards. We shall reject these since our model assumes radiation incident at $z=0$ and forward propagating, in the absence of reflections at the output. Hence the associated amplitudes, proportional to $B(x_6)$ and $B(x_5)$, must vanish. This provides two conditions which can be used to eliminate $a_1'(0)$ and $a_2'(0)$ from Eq. (53). When this is done, and one recognizes that the other roots of interest lie close to $x=1$, there results (correct to lowest significant order in all the small parameters)

$$B(x)=4[(x-\mu)^2-\delta^2-\delta^2\xi^2]\times[i(1-x)a_2(0)+x_0a_1(0)-\tfrac{1}{2}\gamma u_{0z}\hat{a}]\,. \tag{59}$$

When

$$x_0(1+\xi^2)/2\gamma^2-x_0\gg\tfrac{1}{2}\xi^2\delta^2\,, \tag{60}$$

it follows from Eq. (50) that the remaining four roots are well approximated by

$$x_1=\mu+\delta\,,\quad x_2=\mu-\delta\,,\qquad x_3=1+x_0\,,\quad x_4=1-x_0\,, \tag{61}$$

and on employing Eqs. (42)–(44), (52), and (56) and its counterparts for a_1 and a_3 there results after considerable algebra the lowest-significant-order result, on setting $\hat{a}=0$ for simplicity,

$$E_x=\mathrm{Re}\left[-a_2(0)\exp\left(i\frac{\omega}{c}(z-ct)\right)+\tfrac{1}{2}i\xi^2\delta[a_2(0)+ia_1(0)]\frac{\sin(\omega z\delta/c)}{\mu-1-x_0}\times\exp\left(i\frac{\omega}{c}[z(\mu-x_0)-ct]\right)\right]\,, \tag{62}$$

$$E_y=\mathrm{Re}\left[a_1(0)\exp\left(i\frac{\omega}{c}(z-ct)\right)-\tfrac{1}{2}\xi^2\delta[a_2(0)+ia_1(0)]\frac{\sin(\omega z\delta/c)}{\mu-1-x_0}\times\exp\left(i\frac{\omega}{c}[z(\mu-x_0)-ct]\right)\right]\,, \tag{63}$$

$$E_z\simeq 0\,. \tag{64}$$

Note that if the interaction length $L\ll c/\omega\delta$, then in order of magnitude the ratio in Eqs. (62) and (63) of the plasma correction terms, which involve δ, to the vacuum propagation terms, which do not, is roughly

$$\frac{\xi^2\delta}{2}\frac{\omega L\delta/c}{\mu-1-x_0}\lesssim\frac{\xi^2\delta}{2}\frac{\omega L}{c}\approx\frac{\xi^2}{2}\frac{\omega_p L}{c}\frac{1}{\gamma^{3/2}}\,, \tag{65}$$

since $|\mu-1-x_0|\gtrsim\delta$ for the roots in question. Equations (62) and (63) are transverse electric field amplitudes which evolve by the spatial interference of the four independently propagating waves, each with a slightly different wavelength. Constructive interference results in net amplitude enhancement; destructive interference results in net amplitude reduction. Counterparts to these equations for the temporal interference (beating) of oscillations on a free-electron laser have been previously discussed.[11] For either linear or circular polarization for the field at the boundary $z=0$, Eqs. (62) and (63) show that the component of the propagating field proportional to δ is circularily polarized. We shall show below that Eqs. (62) and (63) have only limited utility; they do not appear to apply to the Stanford amplifier experiment, for example, as shall be shown in Sec. III, since the wavelength range of greatest interest is outside of the range of inequality (60).

When $|\mu-1-x_0|\lesssim\delta$ it is readily shown that there is one root

$$x_4\simeq b-x_0-\tfrac{1}{4}\xi^2\delta^2\,, \tag{66}$$

which is well separated from the other three provided that $\delta\ll x_0\ll 1$, and these latter can be got from (55) on retaining on the right only the term with denominator $x-(b+x_0)$. The resulting approximate dispersion relation is

$$[(x-\mu)^2-\delta^2][x-(b+x_0)]+\tfrac{1}{2}\xi^2\delta^2x_0=0\,. \tag{67}$$

This reduced dispersion relation has been given previously.[1] Application of the formulas for the roots of a cubic indicates that Eq. (67) possesses an unstable root, when $\delta\ll x_0\ll 1$, for

$$-\tfrac{1}{2}\xi^2x_0<b+x_0-\mu<(27\delta^2\xi^2x_0/8)^{1/3}\,. \tag{68}$$

This corresponds approximately to

$$(1+\xi^2)/2\gamma^2(1+\tfrac{1}{2}\xi^2)<k_0/k<(1+\xi^2)/2\gamma^2\,,$$

the wavelength range of greatest interest for free-electron lasers. Note that the unstable domain disappears as x_0 vanishes and hence was not found in the geometric optics approximation.[10] The maximum spatial growth rate occurs when

$$b+x_0-\mu=(\tfrac{1}{2}\delta^2\xi^2x_0)^{1/2}$$

and to the requisite accuracy the roots are

$$x_1 = \mu + (\tfrac{1}{2}\delta^2\xi^2 x_0)^{1/3}\exp(-\pi i/3)\,,$$
$$x_2 = x_1^*\,, \tag{69}$$
$$x_3 = \mu - (\tfrac{1}{2}\delta^2\xi^2 x_0)^{1/3}\,.$$

Thus employing Eq. (59) with $\hat{a}=0$, we find to lowest order

$$a_2(z) = \tfrac{1}{2}[a_2(0) - a_1(0)]\exp\left(i\frac{\omega}{c}z x_4\right) + \tfrac{1}{6}[a_2(0) + i a_1(0)]\sum_{j=1}^{3}\exp\left(i\frac{\omega}{c}z x_j\right)\,. \tag{70}$$

Note that

$$\sum_{j=1}^{3}(x_j-\mu) = 0\,,\quad \sum_{j=1}^{3}(x_j-\mu)^2 = 0\,,$$

and

$$\sum_{j=1}^{3}(x_j-\mu)^3 = -\tfrac{1}{2}\delta^2\xi^2 x_0\,, \tag{71}$$

whence the sum in Eq. (70) can be written on Taylor expansion and use of Eq. (71),

$$\sum_{j=1}^{3}\exp\left(i\frac{\omega}{c}z x_j\right) = \exp\left(i\frac{\omega}{c}z\mu\right)\sum_{j=1}^{3}\exp\left(i\frac{\omega}{c}z(x_j-\mu)\right) = \exp\left(i\frac{\omega}{c}z\mu\right)\sum_{n=0}^{\infty}3\frac{[i(\omega/2c)z\delta^2\xi^2 x_0]^{3n}}{(3n)!}\,. \tag{72}$$

Clearly where $(\omega/2c)z\delta^2\xi^2 x_0 \lesssim 1$ the interference of the three modes is important, and only when $(\omega/2c)z\delta^2\xi^2 x_0 \gg 1$ does the spatially unstable mode corresponding to x_1 dominate. Moreover, Eq. (70) shows that the exponentially growing term only has about 1/6 the initial amplitude. This corresponds to an input power coupling loss of 1/36, or −15.56 dB. Such an input coupling loss is well known in traveling-wave tube theory, where only one mode grows exponentially while two or more others do not.[12]

The wave polarization in the unstable regime is also transverse. This is seen from the governing differential equations (35)–(37). If we write

$$a_1(z) = \sum_{j=1}^{4}A(x_j)e^{i\omega x_j z/c}$$

and (73)

$$a_3(z) = \sum_{j=1}^{4}C(x_j)e^{i\omega x_j z/c}\,,$$

then it is a simple matter to show that

$$\frac{|A(x_j)|}{|B(x_j)|} = \frac{2x_0 x_j}{b^2 - x_0^2 - x_j^2} \simeq 1 \tag{74}$$

and

$$\frac{|C(x_j)|}{|B(x_j)|} = \left(\frac{\omega_p}{\omega}\right)^{4/3}\xi^{1/3}(1+\xi^2)^{2/3}\gamma^{-7/3} \ll 1\,. \tag{75}$$

It has been fashionable to describe the gain mechanism for the free-electron laser in terms of parametric coupling between longitudinally polarized beam modes and transversely polarized electromagnetic modes. Indeed, if the helical magnetic pump field is absent ($\xi=0$) then Eq. (50) corresponds to the product of uncoupled dispersion relations for these entities. A ponderomotive force is said to give axial bunching which drives the instability.[1] But, as we have shown, the polarization of the modes on the beam in the presence of the helical pump field is nearly transverse when the growth mechanism is most active, and thus the waves have little associated space change ($\nabla\cdot\vec{E}\simeq 0$); therefore it is clear that the conventional modes have lost their identity in the regime of instability. Indeed, as seen from Fig. 1, one of the transverse waves has a phase velocity below c. As we have stated, Eqs. (62) and (63) describe an interference phenomenon giving small growth and decay alternatively as free-running transverse waves drive transverse electron perturbations which beat in phase against one another. In contrast, Eqs. (70)–(73) describe a steadily accumulating *bunching in phase*, in the regime of complex roots, with a relative phase value such that work is done by the electrons on the wave causing it to grow. Axial bunching (accompanied by an axial electric field E_z) is of higher order in δ.

III. RESULTS

In this section we present some numerical results for the steady-state spatial evolution of the electromagnetic disturbance on the electron beam, assuming the driving fields $a_1(0)$ and $a_2(0)$ at the boundary $z=0$ to be assigned. Values of the physical parameters have been chosen in two distinct classes: those corresponding to a low-current high-energy beam, and those corresponding to a high-current low-energy beam. As in the analysis of Sec. II, the beam is assumed cold and effects of finite radius are not included. The beam is also modeled as having an axially uniform equilibrium. In some experiments, the beam is actually injected as a sequence of short bursts;[2,3] this feature could complicate a detailed comparison between this theory and the observed measurements.

The high-energy results are shown graphically in Figs. 3–7. In Figs. 3–6 are plotted power gain versus axial distance for the transverse electric field component $a_2(z)$ from (54), with the ampli-

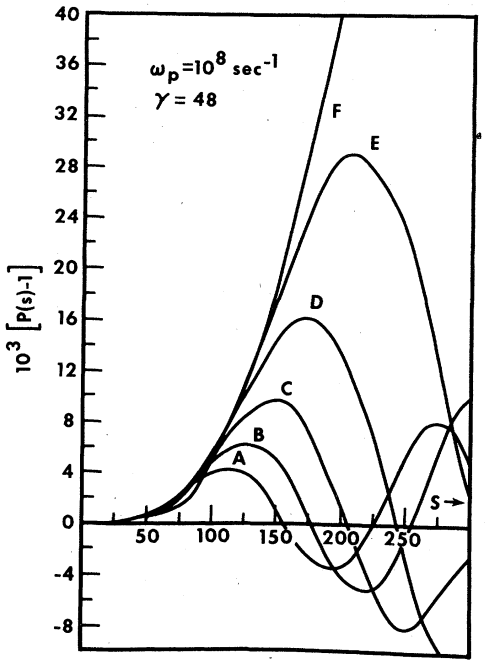

FIG. 3. Power gain vs interaction distance s (measured in units of helical pump period) for (A) $\lambda = 10.575\ \mu$, (B) $\lambda = 10.567\ \mu$, (C) $\lambda = 10.599\ \mu$, (D) $\lambda = 10.551\ \mu$, (E) $\lambda = 10.543\ \mu$, and (F) $\lambda = 10.535\ \mu$. $\omega_p = 10^8$ sec^{-1}, $\gamma = 48$, $\xi = 0.716$, and $k_0 = 1.96$ cm^{-1}. The dispersion relation has six real roots for these cases.

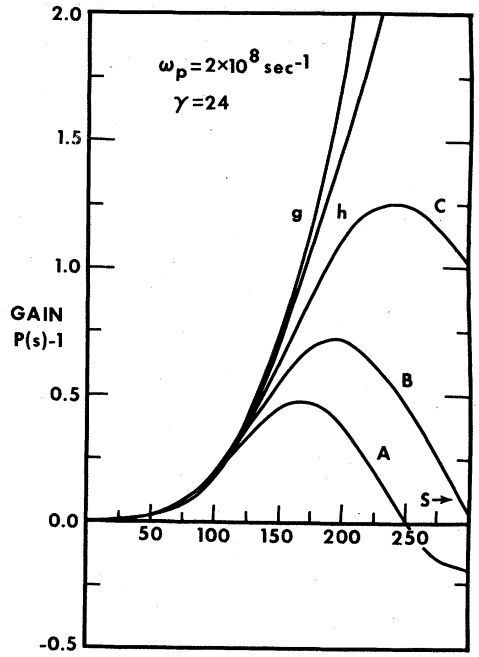

FIG. 5. Power gain vs interaction distance s for (g) $\lambda = 42.155\ \mu$, (h) $\lambda = 42.175\ \mu$ (four real roots, two c.c. roots); (C) $\lambda = 42.195\ \mu$, (B) $\lambda = 42.215\ \mu$, (A) $\lambda = 42.235\ \mu$ (six real roots). $\omega_p = 2\times10^8$ sec^{-1}, $\gamma = 24$, $\xi = 0.716$, and $k_0 = 1.96$ cm^{-1}.

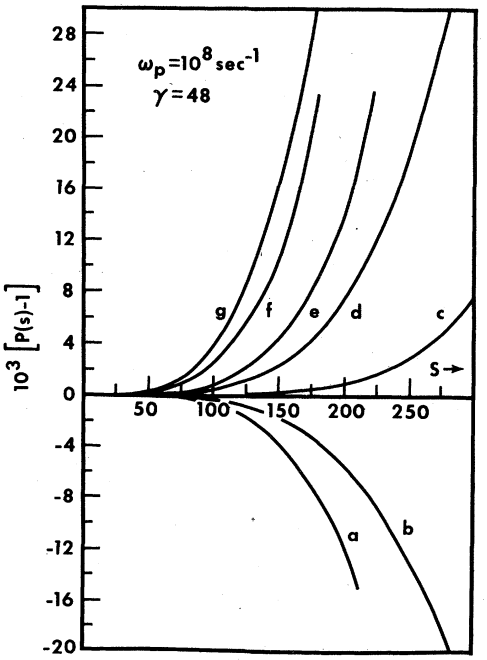

FIG. 4. Power gain vs interaction distance s for (a) $\lambda = 10.503\ \mu$, (b) $\lambda = 10.505\ \mu$, (c) $\lambda = 10.507\ \mu$, (d) $\lambda = 10.509\ \mu$, (e) $\lambda = 10.511\ \mu$, (f) $\lambda = 10.519\ \mu$, and (g) $\lambda = 10.527\ \mu$. $\omega_p = 10^8$ sec^{-1}, $\gamma = 48$, $\xi = 0.716$, and $k_0 = 1.96$ cm^{-1}. The dispersion relation has four real roots and two complex conjugate roots for these cases.

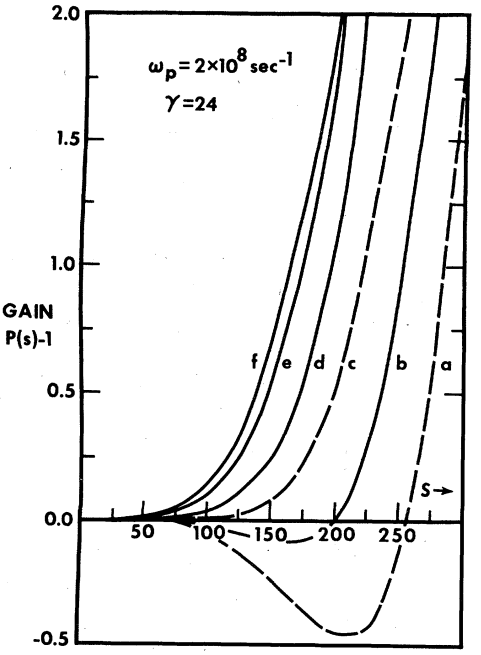

FIG. 6. Power gain vs interaction distance s for (a) $\lambda = 41.995\ \mu$, (b) $\lambda = 42.015\ \mu$, (c) $\lambda = 41.035\ \mu$, (d) $\lambda = 42.055\ \mu$, (e) $\lambda 142.075\ \mu$, (f) $\lambda = 42.095\ \mu$ (four real roots, two c.c. roots). $\omega_p = 2\times10^8$ sec^{-1}, $\gamma = 24$, $\xi = 0.716$, $k_0 = 1.96$ cm^{-1}.

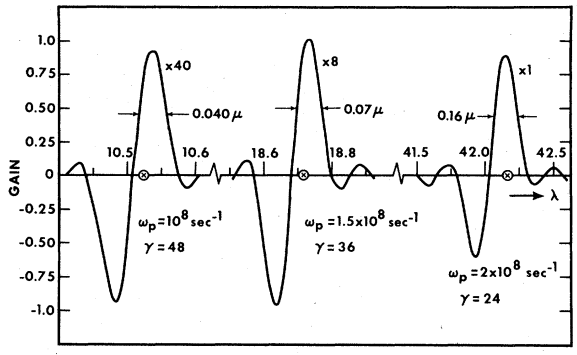

FIG. 7. Gain vs wavelength evaluated at $s=160$ (interaction length 520 cm) for $k_0=1.96$ cm^{-1} and $\xi=0.716$ for three values of ω_p and γ. The FWHM (linewidth) for each curve is 0.38%. The peak gain values are 2.3% ($\lambda=10.520\ \mu$), 12.5% ($\lambda=18.73\ \mu$), and 88% ($\lambda=42.135\ \mu$). The symbol × on the ordinate is the point where the roots of the dispersion relation switch from all six real (longer wavelength side) to four real and two complex (shorter wavelength side). In each case shown, the gain curve embraces the regimes of *both* real and complex roots, corresponding to gain on a stable system due to constructive spatial interference and to exponential growth on an unstable system.

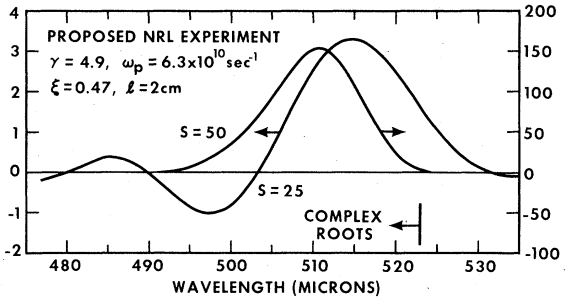

FIG. 8. Gain vs wavelength for conditions of a proposed experiment at the Naval Research Laboratory (Ref. 5). The beam energy is to be 2.0 MV ($\gamma=4.9$), beam current is to be 1.7 kA ($J=6000$A/cm^2), pump period 2.0 cm ($k_0=$cm^{-1}) and pump strength parameter $\xi=0.47$. Results are shown for two interaction lengths, 50 and 100 cm, corresponding to $s=25$ and $s=50$. Peak gain values are 4.23 and 2.64% of what would be predicted for exponential growth of the unstable mode propagating alone.

tudes given by (53); we have taken $a_2(0)=1$ and $a_1(0)=0$. The quantity $P(s)$ is $a_2(z)a_2^*(z)$ and $P(s)-1$ is then the power gain. The axial coordinate s is distance measured in units of the helical magnetic pump period, i.e., $s=k_0z/2\pi$. Except for phase factors, the power in the mode with transverse electric field compoent $a_1(z)$ is approximately equal to that corresponding to $a_2(z)$ [see Eq. (74)]. The power in the longitudinal wave is much smaller [see Eq. (75)]. Thus overall gain could be as large as four times that shown in the figures.

The parameters chosen for the examples presented in Figs. 3–7 are $k_0=1.96$ cm^{-1}, $\xi=0.716$, $\omega_p=10^8$, 1.5×10^8, and 2×10^8 sec^{-1} (corresponding to beam current densities of 15, 34, and 60 mA/cm^2), and $\gamma=48$, 36, and 24. The parameter $s=k_0z/2\pi$ runs from 0 to 300. The individual curves in Figs. 3–6 are for fixed values of the radiation wavelength; capital letter labels designate solutions in the regime of real roots to the dispersion relation (67), while lower-case labels designate solutions in the regime of complex roots. Curves A–F in Fig. 3 are for wavelengths from 10.575 μ to 10.535 μ, respectively, in steps of 0.008 μ. Curves g, f, and e in Fig. 4 are for wavelengths from 10.527 to 10.511 μ in steps of 0.008 μ; curves d–a are for wavelengths of from 10.509 μ to 10.503 μ in steps of 0.002 μ. Figs. 3 and 4 show the change in the nature of the gain versus distance curves as wavelength is varied. At the longer wavelengths (Fig. 3), where the dispersion relation exhibits real roots, the gain alternates between positive and negative values as the spatially propagating modes beat against one another. At $s=160$ (corresponding to an interaction length of 520 cm) the maximum achievable gain for the mode given by $a_2(z)$ is 2.3%. For wavelengths below 10.520 μ the dispersion relation has complex roots, one corresponding to spatial amplification; thus the curves for gain can exhibit monotone behavior (Fig. 4). This example is for parameters resembling those for the reported amplifier experiment,[3] except for the aforementioned complication due to the pulsed nature of the beam in the experiments, with which we have not attempted to deal. The measured power gain was 7% for a circularily polarized incident incident wave, in fair agreement with four times our calculated value of 2.3%, which was for a linearly polarized incident wave. The measured $1/e$ full linewidth was 0.4%, in fair agreement with our calculated FWHM of 0.38% (see Fig. 7).

Figs. 5 and 6 are similar to Figs. 3 and 4, except that $\gamma=24$ and $\omega_p=2\times10^8$ sec^{-1}. Curves A, B, and C (real roots) are for wavelengths of 42.235, 42.215, and 42.195 μ, respectively, while curves a–h are for wavelengths between 41.995 and 42.175 μ, in steps of 0.020 μ. The maximum gain of 88% for $s=160$ occurs at $\lambda=42.135\ \mu$ and is in the regime of complex roots. The FWHM for the gain curve at $s=160$ (rightmost curve in Fig. 7) is also 0.38%. Also shown in Fig. 7 is a gain curve for $\gamma=36$ and $\omega_p=1.5\times10^8$ sec^{-1}, values intermediate to the other two cases. Here maximum gain of 12.5% occurs at $\lambda=18.73\ \mu$ with a FWHM also of 0.38%. All three curves in Fig. 7 have similar shape, equal FWHM's, and similar spanning of the regimes of both real and complex roots to the

dispersion relation.

Fig. 8 shows two gain curves for parameters of an experiment planned at the Naval Research Laboratory.[5] Here a low-energy ($\gamma = 4.9$) intense electron beam ($J = 6000$ A/cm^2) is to be used. The other parameters are $\xi = 0.47$ and $k_0 = \pi$ cm^{-1}. Two interaction lengths, 50 and 100 cm, are considered, corresponding to $s = 25$ and $s = 50$. For $s = 25$, the spatial beating of the modes is clearly in evidence for wavelengths below 505 μ, even though this is within the regime of complex roots. The maximum gain, at $\lambda = 515$ μ is 3.3 (330%). For $s = 50$, the gain curve has slightly lopsided Gaussian shape with a maximum gain of 165 at $\lambda = 511$ μ. The FWHM for $s = 50$ is 2.5%. The e-fold length for the one mode exhibiting growth in this case is 22.88 cm. If pure exponential gain were assumed, one would find for the power gain values of 78 and 6250 for $s = 25$ and 50. The correct analysis is seen to give values which are 4.23 and 2.64% of these, corresponding to coupling losses of 13.7 and 15.8 dB, respectively. The latter value is in close agreement with $1/36 = -15.6$ dB, as discussed above.

IV. ACKNOWLEDGMENTS

Appreciation is extended to Dr. Lazar Friedland for numerical evaluations presented in Figs. 3–8. The efforts of Ira B. Bernstein were supported by the National Science Foundation.

[1]For a review of past work, together with a substantial list of references, see P. Sprangle, R. A. Smith, and V. L. Granatstein, *Free Electron Lasers and Stimulated Scattering from Relativistic Electron Beams*, in *Infrared and Millimeter Waves*, edited by K. Button (Academic, New York, to be published).
[2]L. R. Elias *et al.*, Phys. Rev. Lett. 36, 717 (1976).
[3]D. A. G. Deacon *et al.*, Phys. Rev. Lett. 38, 892 (1977).
[4]D. B. McDermott *et al.*, Phys. Rev. Lett. 41, 1368 (1978).
[5]V. L. Granatstein (private communication).
[6]J. M. J. Madey, Bull. Am. Phys. Soc. 24, 30 (1979).
[7]J. J. Degan, Appl. Phys. 11, 1 (1976).
[8]A. Hasegawa, Bell System Tech. J. 57, 3069 (1978).
[9]N. M. Kroll and W. A. McMullen, Phys. Rev. A 17, 300 (1978).
[10]I. B. Bernstein and J. L. Hirshfield, Phys. Rev. Lett. 40, 761 (1978).
[11]F. A. Hopf *et al.*, Opt. Commun. 18, 413 (1976).
[12]J. R. Pierce, *Traveling-Wave Tubes* (Van Nostrand, Princeton, 1950).